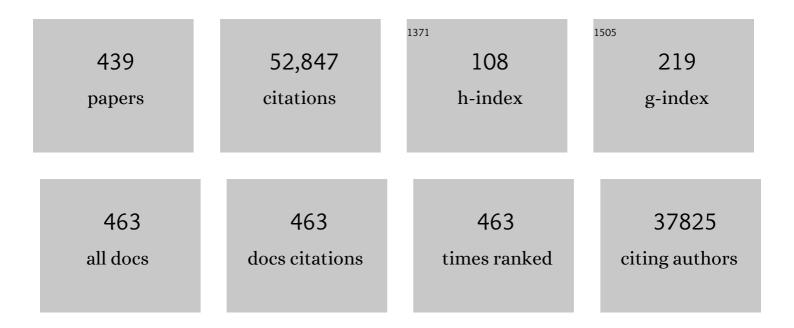
Liberato Manna

List of Publications by Year in descending order

Source: https://exaly.com/author-pdf/9281924/publications.pdf Version: 2024-02-01



#	Article	IF	CITATIONS
1	Bottom-up synthesis of nanosized objects. , 2022, , 85-123.		1
2	Mixed Dimethylammonium/Methylammonium Lead Halide Perovskite Crystals for Improved Structural Stability and Enhanced Photodetection. Advanced Materials, 2022, 34, e2106160.	21.0	18
3	The Reactivity of CsPbBr ₃ Nanocrystals toward Acid/Base Ligands. ACS Nano, 2022, 16, 1444-1455.	14.6	33
4	Red-emissive nanocrystals of Cs ₄ Mn _{<i>x</i>} Cd _{1â^'<i>x</i>} Sb ₂ Cl ₁₂ layered perovskites. Nanoscale, 2022, 14, 305-311.	5.6	6
5	Control of electronic band profiles through depletion layer engineering in core–shell nanocrystals. Nature Communications, 2022, 13, 537.	12.8	27
6	Exploiting the Transformative Features of Metal Halides for the Synthesis of CsPbBr ₃ @SiO ₂ Core–Shell Nanocrystals. Chemistry of Materials, 2022, 34, 405-413.	6.7	29
7	Recent Progress in Halide Perovskite Radiation Detectors for Gamma-Ray Spectroscopy. ACS Energy Letters, 2022, 7, 1066-1085.	17.4	47
8	Magnetic Transitions and Energy Transfer Processes in Sb-Based Zero-Dimensional Metal Halide Nanocrystals Doped with Manganese. ACS Energy Letters, 2022, 7, 1566-1573.	17.4	21
9	Colloidal Bismuth Chalcohalide Nanocrystals. Angewandte Chemie, 2022, 134, .	2.0	5
10	Colloidal Bismuth Chalcohalide Nanocrystals. Angewandte Chemie - International Edition, 2022, 61, .	13.8	17
11	Stable CsPbBr ₃ Nanoclusters Feature a Disk-like Shape and a Distorted Orthorhombic Structure. Journal of the American Chemical Society, 2022, 144, 5059-5066.	13.7	16
12	Transition metal dichalcogenides as catalysts for the hydrogen evolution reaction: The emblematic case of "inert―ZrSe ₂ as catalyst for electrolyzers. Nano Select, 2022, 3, 1069-1081.	3.7	6
13	Topochemical Transformation of Two-Dimensional VSe ₂ into Metallic Nonlayered VO ₂ for Water Splitting Reactions in Acidic and Alkaline Media. ACS Nano, 2022, 16, 351-367.	14.6	23
14	Halide perovskites and perovskite related materials for particle radiation detection. Nanoscale, 2022, 14, 6743-6760.	5.6	17
15	Cesium Manganese Bromide Nanocrystal Sensitizers for Broadband Vis-to-NIR Downshifting. ACS Energy Letters, 2022, 7, 1850-1858.	17.4	30
16	ZnCl ₂ Mediated Synthesis of InAs Nanocrystals with Aminoarsine. Journal of the American Chemical Society, 2022, 144, 10515-10523.	13.7	21
17	Fast Aâ€Site Cation Crossâ€Exchange at Room Temperature: Singleâ€to Double―and Tripleâ€Cation Halide Perovskite Nanocrystals. Angewandte Chemie - International Edition, 2022, 61, .	13.8	29
18	Generation of Free Carriers in MoSe ₂ Monolayers Via Energy Transfer from CsPbBr ₃ Nanocrystals. Advanced Optical Materials, 2022, 10, .	7.3	7

#	Article	IF	CITATIONS
19	Recent Progress in Mixed Aâ€6ite Cation Halide Perovskite Thinâ€Films and Nanocrystals for Solar Cells and Lightâ€Emitting Diodes. Advanced Optical Materials, 2022, 10, .	7.3	47
20	Halide perovskites as disposable epitaxial templates for the phase-selective synthesis of lead sulfochloride nanocrystals. Nature Communications, 2022, 13, .	12.8	16
21	Leadâ€Free Double Perovskite Cs ₂ AgInCl ₆ . Angewandte Chemie, 2021, 133, 11696-11707.	2.0	36
22	Leadâ€Free Double Perovskite Cs ₂ AgInCl ₆ . Angewandte Chemie - International Edition, 2021, 60, 11592-11603.	13.8	168
23	Are There Good Alternatives to Lead Halide Perovskite Nanocrystals?. Nano Letters, 2021, 21, 6-9.	9.1	44
24	Aging of Self-Assembled Lead Halide Perovskite Nanocrystal Superlattices: Effects on Photoluminescence and Energy Transfer. ACS Nano, 2021, 15, 650-664.	14.6	46
25	Synthesis of yolk–shell Co ₃ O ₄ /Co _{1â^x} Ru _x O ₂ microspheres featuring an enhanced electrocatalytic oxygen evolution activity in acidic medium. Journal of Materials Chemistry A. 2021. 9. 10385-10392.	10.3	11
26	Halide Perovskite–Lead Chalcohalide Nanocrystal Heterostructures. Journal of the American Chemical Society, 2021, 143, 1435-1446.	13.7	55
27	Multilayer Diffraction Reveals That Colloidal Superlattices Approach the Structural Perfection of Single Crystals. ACS Nano, 2021, 15, 6243-6256.	14.6	29
28	Mechanical switching of orientation-related photoluminescence in deep-blue 2D layered perovskite ensembles. Nanoscale, 2021, 13, 3948-3956.	5.6	4
29	Low-Temperature Molten Salts Synthesis: CsPbBr ₃ Nanocrystals with High Photoluminescence Emission Buried in Mesoporous SiO ₂ . ACS Energy Letters, 2021, 6, 900-907.	17.4	68
30	0D Nanocrystals as Lightâ€Driven, Localized Chargeâ€Injection Sources for the Contactless Manipulation of Atomically Thin 2D Materials. Advanced Photonics Research, 2021, 2, 2000151.	3.6	9
31	Fluorination suppresses thermal quenching in perovskite QLEDs. Science China Chemistry, 2021, 64, 1113-1114.	8.2	0
32	Reversible Emission Tunability from 2Dâ€Layered Perovskites with Conjugated Organic Cations. Advanced Photonics Research, 2021, 2, 2100005.	3.6	10
33	Engineering the Optical Emission and Robustness of Metalâ€Halide Layered Perovskites through Ligand Accommodation. Advanced Materials, 2021, 33, e2008004.	21.0	23
34	Why Do We Care about Studying Transformations in Inorganic Nanocrystals?. Accounts of Chemical Research, 2021, 54, 1543-1544.	15.6	13
35	Intrinsic and Extrinsic Exciton Recombination Pathways in AgInS ₂ Colloidal Nanocrystals. Energy Material Advances, 2021, 2021, .	11.0	15
36	Sb-Doped Metal Halide Nanocrystals: A 0D versus 3D Comparison. ACS Energy Letters, 2021, 6, 2283-2292.	17.4	83

#	Article	IF	CITATIONS
37	Hollowing of MnO Nanocrystals Triggered by Metal Cation Replacement: Implications for the Electrocatalytic Oxygen Evolution Reaction. ACS Applied Nano Materials, 2021, 4, 5904-5911.	5.0	8
38	State of the Art and Prospects for Halide Perovskite Nanocrystals. ACS Nano, 2021, 15, 10775-10981.	14.6	705
39	Electrochemical p-Doping of CsPbBr ₃ Perovskite Nanocrystals. ACS Energy Letters, 2021, 6, 2519-2525.	17.4	26
40	Understanding Thermal and Aâ€Thermal Trapping Processes in Lead Halide Perovskites Towards Effective Radiation Detection Schemes. Advanced Functional Materials, 2021, 31, 2104879.	14.9	20
41	Switchable Anion Exchange in Polymer-Encapsulated APbX ₃ Nanocrystals Delivers Stable All-Perovskite White Emitters. ACS Energy Letters, 2021, 6, 2844-2853.	17.4	34
42	Guidelines for the characterization of metal halide nanocrystals. Trends in Chemistry, 2021, 3, 631-644.	8.5	9
43	Detection of Pb ²⁺ traces in dispersion of Cs ₄ PbBr ₆ nanocrystals by <i>in situ</i> liquid cell transmission electron microscopy. Nanoscale, 2021, 13, 2317-2323.	5.6	2
44	Metamorphoses of Cesium Lead Halide Nanocrystals. Accounts of Chemical Research, 2021, 54, 498-508.	15.6	39
45	Isolated [SbCl ₆] ^{3–} Octahedra Are the Only Active Emitters in Rb ₇ Sb ₃ Cl ₁₆ Nanocrystals. ACS Energy Letters, 2021, 6, 3952-3959.	17.4	15
46	Fast Intrinsic Emission Quenching in Cs ₄ PbBr ₆ Nanocrystals. Nano Letters, 2021, 21, 8619-8626.	9.1	16
47	Methylammonium Governs Structural and Optical Properties of Hybrid Lead Halide Perovskites through Dynamic Hydrogen Bonding. Chemistry of Materials, 2021, 33, 8524-8533.	6.7	14
48	Structure and Surface Passivation of Ultrathin Cesium Lead Halide Nanoplatelets Revealed by Multilayer Diffraction. ACS Nano, 2021, 15, 20341-20352.	14.6	17
49	Atmosphere-Induced Transient Structural Transformations of Pd–Cu and Pt–Cu Alloy Nanocrystals. Chemistry of Materials, 2021, 33, 8635-8648.	6.7	3
50	Core/Shell CdSe/CdS Bone‣haped Nanocrystals with a Thick and Anisotropic Shell as Optical Emitters. Advanced Optical Materials, 2020, 8, 1901463.	7.3	12
51	Locating and Controlling the Zn Content in In(Zn)P Quantum Dots. Chemistry of Materials, 2020, 32, 557-565.	6.7	40
52	Cs ₃ Cu ₄ In ₂ Cl ₁₃ Nanocrystals: A Perovskite-Related Structure with Inorganic Clusters at A Sites. Inorganic Chemistry, 2020, 59, 548-554.	4.0	16
53	Hidden in Plain Sight: The Overlooked Influence of the Cs ⁺ Substructure on Transformations in Cesium Lead Halide Nanocrystals. ACS Energy Letters, 2020, 5, 3409-3414.	17.4	34
54	Colloidal Bi-Doped Cs ₂ Ag _{1–<i>x</i>} Na _{<i>x</i>} InCl ₆ Nanocrystals: Undercoordinated Surface Cl Ions Limit their Light Emission Efficiency. , 2020, 2, 1442-1449.		41

#	Article	IF	CITATIONS
55	Robustness to High Temperatures of Al ₂ O ₃ -Coated CsPbBr ₃ Nanocrystal Thin Films with High-Photoluminescence Quantum Yield for Light Emission. ACS Applied Nano Materials, 2020, 3, 8167-8175.	5.0	26
56	Microwaveâ€Induced Structural Engineering and Pt Trapping in <i>6R</i> â€TaS ₂ for the Hydrogen Evolution Reaction. Small, 2020, 16, e2003372.	10.0	18
57	Alloy CsCd <i>_x</i> Pb _{1–<i>x</i>} Br ₃ Perovskite Nanocrystals: The Role of Surface Passivation in Preserving Composition and Blue Emission. Chemistry of Materials, 2020, 32, 10641-10652.	6.7	45
58	Stable and Size Tunable CsPbBr ₃ Nanocrystals Synthesized with Oleylphosphonic Acid. Nano Letters, 2020, 20, 8847-8853.	9.1	92
59	Impact of local structure on halogen ion migration in layered methylammonium copper halide memory devices. Journal of Materials Chemistry A, 2020, 8, 17516-17526.	10.3	14
60	Bandgap determination from individual orthorhombic thin cesium lead bromide nanosheets by electron energy-loss spectroscopy. Nanoscale Horizons, 2020, 5, 1610-1617.	8.0	8
61	Efficient, fast and reabsorption-free perovskite nanocrystal-based sensitized plastic scintillators. Nature Nanotechnology, 2020, 15, 462-468.	31.5	226
62	Nanocrystals of Lead Chalcohalides: A Series of Kinetically Trapped Metastable Nanostructures. Journal of the American Chemical Society, 2020, 142, 10198-10211.	13.7	34
63	Compositional Tuning of Carrier Dynamics in Cs ₂ Na _{1–<i>x</i>} Ag _{<i>x</i>} BiCl ₆ Double-Perovskite Nanocrystals. ACS Energy Letters, 2020, 5, 1840-1847.	17.4	63
64	Bright Blue Emitting Cu-Doped Cs ₂ ZnCl ₄ Colloidal Nanocrystals. Chemistry of Materials, 2020, 32, 5897-5903.	6.7	63
65	Photoluminescence enhancement and high accuracy patterning of lead halide perovskite single crystals by MeV ion beam irradiation. Journal of Materials Chemistry C, 2020, 8, 9923-9930.	5.5	12
66	Developing Lattice Matched ZnMgSe Shells on InZnP Quantum Dots for Phosphor Applications. ACS Applied Nano Materials, 2020, 3, 3859-3867.	5.0	23
67	Metastable CdTe@HgTe Core@Shell Nanostructures Obtained by Partial Cation Exchange Evolve into Sintered CdTe Films Upon Annealing. Chemistry of Materials, 2020, 32, 2978-2985.	6.7	10
68	Transforming colloidal Cs ₄ PbBr ₆ nanocrystals with poly(maleic) Tj ETQq0 0 0 rgBT /Ove intermediate heterostructures. Chemical Science, 2020, 11, 3986-3995.	erlock 10 ⁻ 7.4	Tf 50 227 Td 59
69	Light-Driven Permanent Charge Separation across a Hybrid Zero-Dimensional/Two-Dimensional Interface. Journal of Physical Chemistry C, 2020, 124, 8000-8007.	3.1	14
70	Composition-, Size-, and Surface Functionalization-Dependent Optical Properties of Lead Bromide Perovskite Nanocrystals. Journal of Physical Chemistry Letters, 2020, 11, 2079-2085.	4.6	37
71	Permanent Lattice Compression of Lead-Halide Perovskite for Persistently Enhanced Optoelectronic Properties. ACS Energy Letters, 2020, 5, 642-649.	17.4	52
72	Octapod-Shaped CdSe Nanocrystals Hosting Pt with High Mass Activity for the Hydrogen Evolution Reaction. Chemistry of Materials, 2020, 32, 2420-2429.	6.7	26

#	Article	IF	CITATIONS
73	What Defines a Halide Perovskite?. ACS Energy Letters, 2020, 5, 604-610.	17.4	228
74	Temperature-Driven Transformation of CsPbBr ₃ Nanoplatelets into Mosaic Nanotiles in Solution through Self-Assembly. Nano Letters, 2020, 20, 1808-1818.	9.1	66
75	Nano- and microscale apertures in metal films fabricated by colloidal lithography with perovskite nanocrystals. Nanotechnology, 2020, 31, 185304.	2.6	2
76	A robust and highly active hydrogen evolution catalyst based on Ru nanocrystals supported on vertically oriented Cu nanoplates. Journal of Materials Chemistry A, 2020, 8, 10787-10795.	10.3	13
77	Superlattices are Greener on the Other Side: How Light Transforms Self-Assembled Mixed Halide Perovskite Nanocrystals. ACS Energy Letters, 2020, 5, 1465-1473.	17.4	46
78	Directional Anisotropy of the Vibrational Modes in 2D-Layered Perovskites. ACS Nano, 2020, 14, 4689-4697.	14.6	69
79	Cation Exchange Protocols to Radiolabel Aqueous Stabilized ZnS, ZnSe, and CuFeS ₂ Nanocrystals with ⁶⁴ Cu for Dual Radio―and Photoâ€Thermal Therapy. Advanced Functional Materials, 2020, 30, 2002362.	14.9	11
80	X-ray ptychographic mode of self-assembled CdSe/CdS octapod-shaped nanocrystals in thick polymers. Journal of Applied Crystallography, 2020, 53, 741-747.	4.5	2
81	Mechanochemical synthesis of inorganic halide perovskites: evolution of phase-purity, morphology, and photoluminescence. Journal of Materials Chemistry C, 2019, 7, 11406-11410.	5.5	58
82	Ruthenium-Decorated Cobalt Selenide Nanocrystals for Hydrogen Evolution. ACS Applied Nano Materials, 2019, 2, 5695-5703.	5.0	28
83	HfN Nanoparticles: An Unexplored Catalyst for the Electrocatalytic Oxygen Evolution Reaction. Angewandte Chemie, 2019, 131, 15610-15616.	2.0	9
84	HfN Nanoparticles: An Unexplored Catalyst for the Electrocatalytic Oxygen Evolution Reaction. Angewandte Chemie - International Edition, 2019, 58, 15464-15470.	13.8	31
85	Emissive Bi-Doped Double Perovskite Cs ₂ Ag _{1–<i>x</i>} Na _{<i>x</i>} InCl ₆ Nanocrystals. ACS Energy Letters, 2019, 4, 1976-1982.	17.4	198
86	Wide-Angle X-ray Diffraction Evidence of Structural Coherence in CsPbBr ₃ Nanocrystal Superlattices. , 2019, 1, 272-276.		45
87	Design of catalytically active porous gold structures from a bottom-up method: The role of metal traces in CO oxidation and oxidative coupling of methanol. Journal of Catalysis, 2019, 375, 279-286.	6.2	6
88	Alkyl Phosphonic Acids Deliver CsPbBr ₃ Nanocrystals with High Photoluminescence Quantum Yield and Truncated Octahedron Shape. Chemistry of Materials, 2019, 31, 9140-9147.	6.7	125
89	Direct Quantification of Cu Vacancies and Spatial Localization of Surface Plasmon Resonances in Copper Phosphide Nanocrystals. , 2019, 1, 665-670.		13
90	Green-Emitting Powders of Zero-Dimensional Cs ₄ PbBr ₆ : Delineating the Intricacies of the Synthesis and the Origin of Photoluminescence. Chemistry of Materials, 2019, 31, 7761-7769.	6.7	62

#	Article	IF	CITATIONS
91	Ultrathin Orthorhombic PbS Nanosheets. Chemistry of Materials, 2019, 31, 8145-8153.	6.7	37
92	Tunable Near-Infrared Localized Surface Plasmon Resonance of F, In-Codoped CdO Nanocrystals. ACS Applied Materials & Interfaces, 2019, 11, 39921-39929.	8.0	31
93	Investigation into the Photoluminescence Red Shift in Cesium Lead Bromide Nanocrystal Superlattices. Journal of Physical Chemistry Letters, 2019, 10, 655-660.	4.6	86
94	Stable Ligand Coordination at the Surface of Colloidal CsPbBr ₃ Nanocrystals. Journal of Physical Chemistry Letters, 2019, 10, 3715-3726.	4.6	77
95	Resurfacing halide perovskite nanocrystals. Science, 2019, 364, 833-834.	12.6	143
96	Large polaron evidence in the ultrafast THz response of Lead-Halide Perovskites. EPJ Web of Conferences, 2019, 205, 04019.	0.3	0
97	Ultrafast THz Probe of Photoinduced Polarons in Lead-Halide Perovskites. Physical Review Letters, 2019, 122, 166601.	7.8	98
98	Simultaneous Cationic and Anionic Ligand Exchange For Colloidally Stable CsPbBr ₃ Nanocrystals. ACS Energy Letters, 2019, 4, 819-824.	17.4	173
99	Fully Inorganic Ruddlesden–Popper Double Cl–I and Triple Cl–Br–I Lead Halide Perovskite Nanocrystals. Chemistry of Materials, 2019, 31, 2182-2190.	6.7	60
100	Simple fabrication of layered halide perovskite platelets and enhanced photoluminescence from mechanically exfoliated flakes. Nanoscale, 2019, 11, 8334-8342.	5.6	31
101	O ₂ as a molecular probe for nonradiative surface defects in CsPbBr ₃ perovskite nanostructures and single crystals. Nanoscale, 2019, 11, 7613-7623.	5.6	35
102	Metal Halide Perovskite Nanocrystals: Synthesis, Post-Synthesis Modifications, and Their Optical Properties. Chemical Reviews, 2019, 119, 3296-3348.	47.7	1,181
103	CsPbX ₃ /SiO _x (X = Cl, Br, I) monoliths prepared <i>via</i> a novel sol–gel route starting from Cs ₄ PbX ₆ nanocrystals. Nanoscale, 2019, 11, 18739-18745.	5.6	23
104	Trap-Mediated Two-Step Sensitization of Manganese Dopants in Perovskite Nanocrystals. ACS Energy Letters, 2019, 4, 85-93.	17.4	92
105	Broadband Defects Emission and Enhanced Ligand Raman Scattering in OD Cs ₃ Bi ₂ I ₉ Colloidal Nanocrystals. Advanced Functional Materials, 2019, 29, 1805299.	14.9	44
106	Revealing Photoluminescence Modulation from Layered Halide Perovskite Microcrystals upon Cyclic Compression. Advanced Materials, 2019, 31, e1805608.	21.0	16
107	Nanosized, Hollow, and Mn-Doped CeO ₂ /SiO ₂ Catalysts via Galvanic Replacement: Preparation, Characterization, and Application as Highly Active Catalysts. ACS Applied Nano Materials, 2018, 1, 1438-1443.	5.0	15
108	Coating Evaporated MAPI Thin Films with Organic Molecules: Improved Stability at High Temperature and Implementation in High-Efficiency Solar Cells. ACS Energy Letters, 2018, 3, 835-839.	17.4	30

#	Article	IF	CITATIONS
109	Zero-Dimensional Cesium Lead Halides: History, Properties, and Challenges. Journal of Physical Chemistry Letters, 2018, 9, 2326-2337.	4.6	210
110	Genesis, challenges and opportunities for colloidal lead halide perovskite nanocrystals. Nature Materials, 2018, 17, 394-405.	27.5	1,632
111	Benzoyl Halides as Alternative Precursors for the Colloidal Synthesis of Lead-Based Halide Perovskite Nanocrystals. Journal of the American Chemical Society, 2018, 140, 2656-2664.	13.7	490
112	Role of Acid–Base Equilibria in the Size, Shape, and Phase Control of Cesium Lead Bromide Nanocrystals. ACS Nano, 2018, 12, 1704-1711.	14.6	395
113	Lateral epitaxial heterojunctions in single nanowires fabricated by masked cation exchange. Nature Communications, 2018, 9, 505.	12.8	28
114	The Crucial Role of the Support in the Transformations of Bimetallic Nanoparticles and Catalytic Performance. ACS Catalysis, 2018, 8, 1031-1037.	11.2	31
115	Generating plasmonic heterostructures by cation exchange and redox reactions of covellite CuS nanocrystals with Au ³⁺ ions. Nanoscale, 2018, 10, 2781-2789.	5.6	28
116	Understanding and tailoring ligand interactions in the self-assembly of branched colloidal nanocrystals into planar superlattices. Nature Communications, 2018, 9, 1141.	12.8	32
117	Planar Double-Epsilon-Near-Zero Cavities for Spontaneous Emission and Purcell Effect Enhancement. ACS Photonics, 2018, 5, 2287-2294.	6.6	65
118	Colloidal CsX (X = Cl, Br, I) Nanocrystals and Their Transformation to CsPbX ₃ Nanocrystals by Cation Exchange. Chemistry of Materials, 2018, 30, 79-83.	6.7	67
119	Exfoliation of Few-Layer Black Phosphorus in Low-Boiling-Point Solvents and Its Application in Li-Ion Batteries. Chemistry of Materials, 2018, 30, 506-516.	6.7	93
120	Ni–Co–S–Se Alloy Nanocrystals: Influence of the Composition on Their in Situ Transformation and Electrocatalytic Activity for the Oxygen Evolution Reaction. ACS Applied Nano Materials, 2018, 1, 5753-5762.	5.0	26
121	The Phosphine Oxide Route toward Lead Halide Perovskite Nanocrystals. Journal of the American Chemical Society, 2018, 140, 14878-14886.	13.7	136
122	Fe ²⁺ Deficiencies, FeO Subdomains, and Structural Defects Favor Magnetic Hyperthermia Performance of Iron Oxide Nanocubes into Intracellular Environment. Nano Letters, 2018, 18, 6856-6866.	9.1	53
123	Shape-Pure, Nearly Monodispersed CsPbBr ₃ Nanocubes Prepared Using Secondary Aliphatic Amines. Nano Letters, 2018, 18, 7822-7831.	9.1	132
124	Effects of Oxygen Plasma on the Chemical, Light-Emitting, and Electrical-Transport Properties of Inorganic and Hybrid Lead Bromide Perovskite Nanocrystal Films. ACS Applied Nano Materials, 2018, 1, 5396-5400.	5.0	8
125	Molecular Iodine for a General Synthesis of Binary and Ternary Inorganic and Hybrid Organic–Inorganic Iodide Nanocrystals. Chemistry of Materials, 2018, 30, 6915-6921.	6.7	36
126	Colloidal Synthesis of Double Perovskite Cs ₂ AgInCl ₆ and Mn-Doped Cs ₂ AgInCl ₆ Nanocrystals. Journal of the American Chemical Society, 2018, 140, 12989-12995.	13.7	397

#	Article	IF	CITATIONS
127	Selective antimony reduction initiating the nucleation and growth of InSb quantum dots. Nanoscale, 2018, 10, 11110-11116.	5.6	11
128	Manipulating the morphology of the nano oxide domain in AuCu–iron oxide dumbbell-like nanocomposites as a tool to modify magnetic properties. RSC Advances, 2018, 8, 22411-22421.	3.6	1
129	The Many "Facets―of Halide Ions in the Chemistry of Colloidal Inorganic Nanocrystals. Chemical Reviews, 2018, 118, 7804-7864.	47.7	209
130	<i>Ab Initio</i> Structure Determination of Cu _{2–<i>x</i>} Te Plasmonic Nanocrystals by Precession-Assisted Electron Diffraction Tomography and HAADF-STEM Imaging. Inorganic Chemistry, 2018, 57, 10241-10248.	4.0	25
131	Iron Oxide Colloidal Nanoclusters as Theranostic Vehicles and Their Interactions at the Cellular Level. Nanomaterials, 2018, 8, 315.	4.1	20
132	In situ LiFePO4 nano-particles grown on few-layer graphene flakes as high-power cathode nanohybrids for lithium-ion batteries. Nano Energy, 2018, 51, 656-667.	16.0	50
133	Triggering Cation Exchange Reactions by Doping. Journal of Physical Chemistry Letters, 2018, 9, 4895-4900.	4.6	12
134	In Situ Dynamic Nanostructuring of the Cu–Ti Catalyst-Support System Promotes Hydrogen Evolution under Alkaline Conditions. ACS Applied Materials & Interfaces, 2018, 10, 29583-29592.	8.0	18
135	Metal-support interaction in catalysis: The influence of the morphology of a nano-oxide domain on catalytic activity. Applied Catalysis B: Environmental, 2018, 237, 753-762.	20.2	14
136	Tuning and Locking the Localized Surface Plasmon Resonances of CuS (Covellite) Nanocrystals by an Amorphous CuPd _{<i>x</i>} S Shell. Chemistry of Materials, 2017, 29, 1716-1723.	6.7	50
137	Colloidal Monolayer β-In ₂ Se ₃ Nanosheets with High Photoresponsivity. Journal of the American Chemical Society, 2017, 139, 3005-3011.	13.7	105
138	<i>In Situ</i> Transmission Electron Microscopy Study of Electron Beam-Induced Transformations in Colloidal Cesium Lead Halide Perovskite Nanocrystals. ACS Nano, 2017, 11, 2124-2132.	14.6	246
139	Nearly Monodisperse Insulator Cs ₄ PbX ₆ (X = Cl, Br, I) Nanocrystals, Their Mixed Halide Compositions, and Their Transformation into CsPbX ₃ Nanocrystals. Nano Letters, 2017, 17, 1924-1930.	9.1	488
140	Plasmonic doped semiconductor nanocrystals: Properties, fabrication, applications and perspectives. Physics Reports, 2017, 674, 1-52.	25.6	252
141	Interplay of Internal Structure and Interfaces on the Emitting Properties of Hybrid ZnO Hierarchical Particles. ACS Applied Materials & Interfaces, 2017, 9, 15182-15191.	8.0	5
142	Role of Nonradiative Defects and Environmental Oxygen on Exciton Recombination Processes in CsPbBr ₃ Perovskite Nanocrystals. Nano Letters, 2017, 17, 3844-3853.	9.1	101
143	Selective Fe Promotion on Au Nanoparticles: An Efficient Way to Activate Au/SiO ₂ Catalysts for the CO Oxidation Reaction. ChemCatChem, 2017, 9, 2952-2960.	3.7	7
144	"Quantized―Doping of Individual Colloidal Nanocrystals Using Size-Focused Metal Quantum Clusters. ACS Nano, 2017, 11, 6233-6242.	14.6	21

#	Article	IF	CITATIONS
145	From CsPbBr ₃ Nano-Inks to Sintered CsPbBr ₃ –CsPb ₂ Br ₅ Films via Thermal Annealing: Implications on Optoelectronic Properties. Journal of Physical Chemistry C, 2017, 121, 11956-11961.	3.1	96
146	Gold–iron oxide dimers for magnetic hyperthermia: the key role of chloride ions in the synthesis to boost the heating efficiency. Journal of Materials Chemistry B, 2017, 5, 4587-4594.	5.8	30
147	Role of the Crystal Structure in Cation Exchange Reactions Involving Colloidal Cu ₂ Se Nanocrystals. Journal of the American Chemical Society, 2017, 139, 9583-9590.	13.7	83
148	Ga for Zn Cation Exchange Allows for Highly Luminescent and Photostable InZnP-Based Quantum Dots. Chemistry of Materials, 2017, 29, 5192-5199.	6.7	50
149	Reversible Concentration-Dependent Photoluminescence Quenching and Change of Emission Color in CsPbBr ₃ Nanowires and Nanoplatelets. Journal of Physical Chemistry Letters, 2017, 8, 2725-2729.	4.6	50
150	Dual Band Electrochromic Devices Based on Nb-Doped TiO ₂ Nanocrystalline Electrodes. ACS Nano, 2017, 11, 3576-3584.	14.6	130
151	Changing the Dimensionality of Cesium Lead Bromide Nanocrystals by Reversible Postsynthesis Transformations with Amines. Chemistry of Materials, 2017, 29, 4167-4171.	6.7	142
152	Strongly emissive perovskite nanocrystal inks for high-voltage solar cells. Nature Energy, 2017, 2, .	39.5	544
153	Colloidal Synthesis of Bipolar Off-Stoichiometric Gallium Iron Oxide Spinel-Type Nanocrystals with Near-IR Plasmon Resonance. Journal of the American Chemical Society, 2017, 139, 1198-1206.	13.7	25
154	Solid State Intercalation, Deintercalation, and Cation Exchange in Colloidal 2D Bi ₂ Se ₃ and Bi ₂ Te ₃ Nanocrystals. Chemistry of Materials, 2017, 29, 1419-1429.	6.7	14
155	Large scale syntheses of colloidal nanomaterials. Nano Today, 2017, 12, 46-63.	11.9	69
156	Bright-Emitting Perovskite Films by Large-Scale Synthesis and Photoinduced Solid-State Transformation of CsPbBr ₃ Nanoplatelets. ACS Nano, 2017, 11, 10206-10213.	14.6	118
157	Fluorescent Alloy CsPb _{<i>x</i>} Mn _{1–<i>x</i>} I ₃ Perovskite Nanocrystals with High Structural and Optical Stability. ACS Energy Letters, 2017, 2, 2183-2186.	17.4	305
158	Doped Halide Perovskite Nanocrystals for Reabsorption-Free Luminescent Solar Concentrators. ACS Energy Letters, 2017, 2, 2368-2377.	17.4	224
159	Postsynthesis Transformation of Insulating Cs ₄ PbBr ₆ Nanocrystals into Bright Perovskite CsPbBr ₃ through Physical and Chemical Extraction of CsBr. ACS Energy Letters, 2017, 2, 2445-2448.	17.4	177
160	Low-Temperature Electron Beam-Induced Transformations of Cesium Lead Halide Perovskite Nanocrystals. ACS Omega, 2017, 2, 5660-5665.	3.5	60
161	Laserâ€Induced Localized Growth of Methylammonium Lead Halide Perovskite Nano―and Microcrystals on Substrates. Advanced Functional Materials, 2017, 27, 1701613.	14.9	38
162	Hollow and Porous Nickel Cobalt Perselenide Nanostructured Microparticles for Enhanced Electrocatalytic Oxygen Evolution. Chemistry of Materials, 2017, 29, 7032-7041.	6.7	93

#	Article	IF	CITATIONS
163	Writing on Nanocrystals: Patterning Colloidal Inorganic Nanocrystal Films through Irradiation-Induced Chemical Transformations of Surface Ligands. Journal of the American Chemical Society, 2017, 139, 13250-13259.	13.7	34
164	From Capacitance-Controlled to Diffusion-Controlled Electrochromism in Nb-Doped TiO ₂ Nanocrystalline Electrodes. ECS Transactions, 2017, 77, 1671-1679.	0.5	6
165	Quasi-Static Resonances in the Visible Spectrum from All-Dielectric Intermediate Band Semiconductor Nanocrystals. Nano Letters, 2017, 17, 7691-7695.	9.1	38
166	AuCu alloy nanoparticles supported on SiO2: Impact of redox pretreatments in the catalyst performance in CO oxidation. Catalysis Today, 2017, 282, 105-110.	4.4	33
167	Fully Solutionâ€Processed Conductive Films Based on Colloidal Copper Selenide Nanosheets for Flexible Electronics. Advanced Functional Materials, 2016, 26, 3670-3677.	14.9	46
168	Ptychographic Imaging of Branched Colloidal Nanocrystals Embedded in Free-Standing Thick Polystyrene Films. Scientific Reports, 2016, 6, 19397.	3.3	8
169	Tic-Tac-Toe Binary Lattices from the Interfacial Self-Assembly of Branched and Spherical Nanocrystals. ACS Nano, 2016, 10, 4345-4353.	14.6	27
170	Semiconducting and optical properties of selected binary compounds by linear response DFT+U and hybrid functional methods. Theoretical Chemistry Accounts, 2016, 135, 1.	1.4	13
171	Colloidal Synthesis of Quantum Confined Single Crystal CsPbBr ₃ Nanosheets with Lateral Size Control up to the Micrometer Range. Journal of the American Chemical Society, 2016, 138, 7240-7243.	13.7	446
172	Tuning the Lattice Parameter of In _{<i>x</i>} Zn _{<i>y</i>} P for Highly Luminescent Lattice-Matched Core/Shell Quantum Dots. ACS Nano, 2016, 10, 4754-4762.	14.6	117
173	Polymer-Free Films of Inorganic Halide Perovskite Nanocrystals as UV-to-White Color-Conversion Layers in LEDs. Chemistry of Materials, 2016, 28, 2902-2906.	6.7	152
174	Influence of the Ion Coordination Number on Cation Exchange Reactions with Copper Telluride Nanocrystals. Journal of the American Chemical Society, 2016, 138, 7082-7090.	13.7	67
175	Assembly of Branched Colloidal Nanocrystals in Polymer Films Leads to Enhanced Viscous Deformation Resistance. Nano Letters, 2016, 16, 6154-6163.	9.1	5
176	Evolution of CsPbBr ₃ nanocrystals upon post-synthesis annealing under an inert atmosphere. Journal of Materials Chemistry C, 2016, 4, 9179-9182.	5.5	62
177	Nonlinear Carrier Interactions in Lead Halide Perovskites and the Role of Defects. Journal of the American Chemical Society, 2016, 138, 13604-13611.	13.7	73
178	Dumbbell-like Au _{0.5} Cu _{0.5} @Fe ₃ O ₄ Nanocrystals: Synthesis, Characterization, and Catalytic Activity in CO Oxidation. ACS Applied Materials & Interfaces, 2016, 8, 28624-28632.	8.0	20
179	Colloidal Synthesis of Strongly Fluorescent CsPbBr ₃ Nanowires with Width Tunable down to the Quantum Confinement Regime. Chemistry of Materials, 2016, 28, 6450-6454.	6.7	219
180	Ultrafast Photodoping and Plasmon Dynamics in Fluorine–Indium Codoped Cadmium Oxide Nanocrystals for All-Optical Signal Manipulation at Optical Communication Wavelengths. Journal of Physical Chemistry Letters, 2016, 7, 3873-3881.	4.6	46

#	Article	IF	CITATIONS
181	Tuning the CO oxidation catalytic activity of supported metal–metal oxide heterostructures by an aqueous phase post-treatment process. Journal of Materials Chemistry A, 2016, 4, 18075-18083.	10.3	9
182	<i>N</i> -Methylformamide as a Source of Methylammonium Ions in the Synthesis of Lead Halide Perovskite Nanocrystals and Bulk Crystals. ACS Energy Letters, 2016, 1, 1042-1048.	17.4	59
183	In situ microscopy of the self-assembly of branched nanocrystals in solution. Nature Communications, 2016, 7, 11213.	12.8	91
184	Selfâ€Assembled Dense Colloidal Cu ₂ Te Nanodisk Networks in P3HT Thin Films with Enhanced Photocurrent. Advanced Functional Materials, 2016, 26, 4535-4542.	14.9	19
185	Beyond Conventional Quantum Dots. ChemPhysChem, 2016, 17, 553-554.	2.1	0
186	Colloidal CuFeS ₂ Nanocrystals: Intermediate Fe d-Band Leads to High Photothermal Conversion Efficiency. Chemistry of Materials, 2016, 28, 4848-4858.	6.7	126
187	Thermal Stability and Anisotropic Sublimation of Two-Dimensional Colloidal Bi ₂ Te ₃ and Bi ₂ Se ₃ Nanocrystals. Nano Letters, 2016, 16, 4217-4223.	9.1	60
188	Effect of Core/Shell Interface on Carrier Dynamics and Optical Gain Properties of Dual-Color Emitting CdSe/CdS Nanocrystals. ACS Nano, 2016, 10, 6877-6887.	14.6	57
189	Cu ₂ Se and Cu Nanocrystals as Local Sources of Copper in Thermally Activated <i>In Situ</i> Cation Exchange. ACS Nano, 2016, 10, 2406-2414.	14.6	23
190	The effect of Au domain size on the CO oxidation catalytic activity of colloidal Au–FeOx dumbbell-like heterodimers. Journal of Catalysis, 2016, 338, 115-123.	6.2	37
191	Au _{1â^x} Cu _x colloidal nanoparticles synthesized via a one-pot approach: understanding the temperature effect on the Au : Cu ratio. RSC Advances, 2016, 6, 22213-22221.	3.6	7
192	Forging Colloidal Nanostructures via Cation Exchange Reactions. Chemical Reviews, 2016, 116, 10852-10887.	47.7	551
193	Co _{<i>x</i>} Fe _{3–<i>x</i>} O ₄ Nanocubes for Theranostic Applications: Effect of Cobalt Content and Particle Size. Chemistry of Materials, 2016, 28, 1769-1780.	6.7	142
194	Relevance of LiPF ₆ as Etching Agent of LiMnPO ₄ Colloidal Nanocrystals for High Rate Performing Li-ion Battery Cathodes. ACS Applied Materials & Interfaces, 2016, 8, 4069-4075.	8.0	20
195	Accelerated Removal of Fe-Antisite Defects while Nanosizing Hydrothermal LiFePO ₄ with Ca ²⁺ . Nano Letters, 2016, 16, 2692-2697.	9.1	52
196	Solution Synthesis Approach to Colloidal Cesium Lead Halide Perovskite Nanoplatelets with Monolayer-Level Thickness Control. Journal of the American Chemical Society, 2016, 138, 1010-1016.	13.7	747
197	Binder-free graphene as an advanced anode for lithium batteries. Journal of Materials Chemistry A, 2016, 4, 6886-6895.	10.3	79
198	X-ray Lithography on Perovskite Nanocrystals Films: From Patterning with Anion-Exchange Reactions to Enhanced Stability in Air and Water. ACS Nano, 2016, 10, 1224-1230.	14.6	320

#	Article	IF	CITATIONS
199	Nanostructures for Photonics. , 2016, , 2827-2843.		0
200	Thermally Driven Cation Exchange at Solid State between Cu2Se and CdSe Nanocrystals: an In-Situ TEM Study. Microscopy and Microanalysis, 2015, 21, 947-948.	0.4	0
201	From Binary Cu ₂ S to Ternary Cu–In–S and Quaternary Cu–In–Zn–S Nanocrystals with Tunable Composition <i>via</i> Partial Cation Exchange. ACS Nano, 2015, 9, 521-531.	14.6	173
202	Hollow Iron Oxide Nanoparticles in Polymer Nanobeads as MRI Contrast Agents. Journal of Physical Chemistry C, 2015, 119, 6246-6253.	3.1	14
203	Plasmonic Copper Sulfide Nanocrystals Exhibiting Near-Infrared Photothermal and Photodynamic Therapeutic Effects. ACS Nano, 2015, 9, 1788-1800.	14.6	536
204	Cu _{3-<i>x</i>} P Nanocrystals as a Material Platform for Near-Infrared Plasmonics and Cation Exchange Reactions. Chemistry of Materials, 2015, 27, 1120-1128.	6.7	137
205	Prospects of Nanoscience with Nanocrystals. ACS Nano, 2015, 9, 1012-1057.	14.6	1,005
206	Nanoscale Transformations of Alumina-Supported AuCu Ordered Phase Nanocrystals and Their Activity in CO Oxidation. ACS Catalysis, 2015, 5, 2154-2163.	11.2	54
207	17.6% stabilized efficiency in low-temperature processed planar perovskite solar cells. Energy and Environmental Science, 2015, 8, 2365-2370.	30.8	300
208	Tuning the Optical Properties of Cesium Lead Halide Perovskite Nanocrystals by Anion Exchange Reactions. Journal of the American Chemical Society, 2015, 137, 10276-10281.	13.7	1,765
209	Band structure engineering via piezoelectric fields in strained anisotropic CdSe/CdS nanocrystals. Nature Communications, 2015, 6, 7905.	12.8	65
210	Cation exchange mediated elimination of the Fe-antisites in the hydrothermal synthesis of LiFePO4. Nano Energy, 2015, 16, 256-267.	16.0	54
211	Cu Vacancies Boost Cation Exchange Reactions in Copper Selenide Nanocrystals. Journal of the American Chemical Society, 2015, 137, 9315-9323.	13.7	174
212	Insights into the Structure of Dot@Rod and Dot@Octapod CdSe@CdS Heterostructures. Journal of Physical Chemistry C, 2015, 119, 16338-16348.	3.1	8
213	High-Efficiency All-Solution-Processed Light-Emitting Diodes Based on Anisotropic Colloidal Heterostructures with Polar Polymer Injecting Layers. Nano Letters, 2015, 15, 5455-5464.	9.1	69
214	Sustainable nanotechnology. Chemical Society Reviews, 2015, 44, 5755-5757.	38.1	29
215	Pyramid-Shaped Wurtzite CdSe Nanocrystals with Inverted Polarity. ACS Nano, 2015, 9, 8537-8546.	14.6	25
216	A sustainable future for photonic colloidal nanocrystals. Chemical Society Reviews, 2015, 44, 5897-5914.	38.1	115

#	Article	IF	CITATIONS
217	Elastomeric Nanocomposite Foams for the Removal of Heavy Metal Ions from Water. ACS Applied Materials & Interfaces, 2015, 7, 14778-14784.	8.0	69
218	Direct Synthesis of Carbon-Doped TiO ₂ –Bronze Nanowires as Anode Materials for High Performance Lithium-Ion Batteries. ACS Applied Materials & Interfaces, 2015, 7, 25139-25146.	8.0	65
219	Nanoscale Transformations in Covellite (CuS) Nanocrystals in the Presence of Divalent Metal Cations in a Mild Reducing Environment. Chemistry of Materials, 2015, 27, 7531-7537.	6.7	89
220	Selective Cation Exchange in the Core Region of Cu _{2–<i>x</i>} Se/Cu _{2–<i>x</i>} S Core/Shell Nanocrystals. Journal of the American Chemical Society, 2015, 137, 12195-12198.	13.7	55
221	Post-Synthesis Incorporation of ⁶⁴ Cu in CuS Nanocrystals to Radiolabel Photothermal Probes: A Feasible Approach for Clinics. Journal of the American Chemical Society, 2015, 137, 15145-15151.	13.7	56
222	Singleâ€Mode Lasing from Colloidal Waterâ€Soluble CdSe/CdS Quantum Dotâ€inâ€Rods. Small, 2015, 11, 1328-1334.	10.0	70
223	Squeezing Terahertz Light into Nanovolumes: Nanoantenna Enhanced Terahertz Spectroscopy (NETS) of Semiconductor Quantum Dots. Nano Letters, 2015, 15, 386-391.	9.1	86
224	Three-dimensional coherent diffractive imaging on non-periodic specimens at the ESRF beamline ID10. Journal of Synchrotron Radiation, 2014, 21, 594-599.	2.4	26
225	Nanoantenna Enhanced Terahertz Spectroscopy of a Monolayer of Cadmium Selenide Quantum Dots. , 2014, , .		0
226	Germanium Nanocrystals-MWCNTs Composites as Anode Materials for Lithium Ion Batteries. ECS Transactions, 2014, 62, 19-24.	0.5	7
227	Iron-oxide colloidal nanoclusters: from fundamental physical properties to diagnosis and therapy. , 2014, , .		2
228	Assembly-mediated interplay of dipolar interactions and surface spin disorder in colloidal maghemite nanoclusters. Nanoscale, 2014, 6, 3764-3776.	5.6	79
229	Self-Assembly of Octapod-Shaped Colloidal Nanocrystals into a Hexagonal Ballerina Network Embedded in a Thin Polymer Film. Nano Letters, 2014, 14, 1056-1063.	9.1	42
230	Oxygen Sensitivity of Atomically Passivated CdS Nanocrystal Films. ACS Applied Materials & Interfaces, 2014, 6, 9517-9523.	8.0	17
231	Hollow and Concave Nanoparticles via Preferential Oxidation of the Core in Colloidal Core/Shell Nanocrystals. Journal of the American Chemical Society, 2014, 136, 9061-9069.	13.7	32
232	New materials for tunable plasmonic colloidal nanocrystals. Chemical Society Reviews, 2014, 43, 3957-3975.	38.1	383
233	Generalized One-Pot Synthesis of Copper Sulfide, Selenide-Sulfide, and Telluride-Sulfide Nanoparticles. Chemistry of Materials, 2014, 26, 1442-1449.	6.7	150
234	Etched Colloidal LiFePO4 Nanoplatelets toward High-Rate Capable Li-Ion Battery Electrodes. Nano Letters, 2014, 14, 6828-6835.	9.1	53

Liberato Manna

1.5

17

#	ARTICLE	IF	CITATIONS
235	Sn Cation Valency Dependence in Cation Exchange Reactions Involving Cu2-xSe Nanocrystals. Journal of the American Chemical Society, 2014, 136, 16277-16284.	13.7	111
236	A theoretical investigation of the (0001) covellite surfaces. Journal of Chemical Physics, 2014, 141, 044702.	3.0	17
237	Charge separation in Pt-decorated CdSe@CdS octapod nanocrystals. Nanoscale, 2014, 6, 2238-2243.	5.6	15
238	Synthesis of highly luminescent wurtzite CdSe/CdS giant-shell nanocrystals using a fast continuous injection route. Journal of Materials Chemistry C, 2014, 2, 3439.	5.5	90
239	The Impact of the Crystallization Processes on the Structural and Optical Properties of Hybrid Perovskite Films for Photovoltaics. Journal of Physical Chemistry Letters, 2014, 5, 3836-3842.	4.6	238
240	Bottom-Up Synthesis of Nanosized Objects. , 2014, , 47-80.		2
241	Nanocrystal Film Patterning by Inhibiting Cation Exchange via Electron-Beam or X-ray Lithography. Nano Letters, 2014, 14, 2116-2122.	9.1	46
242	Redox Centers Evolution in Phospho-Olivine Type (LiFe _{0.5} Mn _{0.5}) Tj ETQq0 0 0 rgBT /C)verlock 1 9.1	0 Tf 50 462 1
243	Alloyed Copper Chalcogenide Nanoplatelets <i>via</i> Partial Cation Exchange Reactions. ACS Nano, 2014, 8, 8407-8418.	14.6	123
244	One pot synthesis of monodisperse water soluble iron oxide nanocrystals with high values of the specific absorption rate. Journal of Materials Chemistry B, 2014, 2, 4426.	5.8	127
245	Continuous-wave biexciton lasing at room temperature using solution-processed quantum wells. Nature Nanotechnology, 2014, 9, 891-895.	31.5	433
246	Antibody-Functionalized Inorganic NPs: Mimicking Nature for Targeted Diagnosis and Therapy. , 2014, , 1-28.		1
247	Cold field emission dominated photoconductivity in ordered three-dimensional assemblies of octapod-shaped CdSe/CdS nanocrystals. Nanoscale, 2013, 5, 7596.	5.6	8
248	Electrical Properties of Nanorods. Nanoscience and Technology, 2013, , 57-85.	1.5	0
249	Magnetic Properties of Nanorods. Nanoscience and Technology, 2013, , 133-213.	1.5	2
250	Catalytic Properties of Nanorods. Nanoscience and Technology, 2013, , 215-240.	1.5	0
251	Synthesis of Uniform Disk-Shaped Copper Telluride Nanocrystals and Cation Exchange to Cadmium Telluride Quantum Disks with Stable Red Emission. Journal of the American Chemical Society, 2013, 135, 12270-12278.	13.7	138

252 Physical Properties of Nanorods. Nanoscience and Technology, 2013, , .

#	Article	IF	CITATIONS
253	Radiofrequency characterization of polydimethylsiloxane – iron oxide based nanocomposites. Microelectronic Engineering, 2013, 111, 46-51.	2.4	10
254	Bragg extraction of light in 2D photonic Thue–Morse quasicrystals patterned in active CdSe/CdS nanorod–polymer nanocomposites. Nanoscale, 2013, 5, 331-336.	5.6	23
255	Culn _{<i>x</i>} Ga _{1–<i>x</i>} S ₂ Nanocrystals with Tunable Composition and Band Gap Synthesized via a Phosphine-Free and Scalable Procedure. Chemistry of Materials, 2013, 25, 3180-3187.	6.7	65
256	GHz Properties of Magnetophoretically Aligned Iron-Oxide Nanoparticle Doped Polymers. ACS Applied Materials & Interfaces, 2013, 5, 2908-2914.	8.0	4
257	Ultrafast Optical Mapping of Nonlinear Plasmon Dynamics in Cu _{2–<i>x</i>} Se Nanoparticles. Journal of Physical Chemistry Letters, 2013, 4, 3337-3344.	4.6	47
258	Copper Sulfide Nanocrystals with Tunable Composition by Reduction of Covellite Nanocrystals with Cu ⁺ Ions. Journal of the American Chemical Society, 2013, 135, 17630-17637.	13.7	377
259	Mobility and Spatial Distribution of Photoexcited Electrons in CdSe/CdS Nanorods. Journal of Physical Chemistry C, 2013, 117, 3146-3151.	3.1	40
260	Single-mode tunable laser emission in the single-exciton regime from colloidal nanocrystals. Nature Communications, 2013, 4, 2376.	12.8	118
261	Colloidal Synthesis of Cuprite (Cu ₂ O) Octahedral Nanocrystals and Their Electrochemical Lithiation. ACS Applied Materials & Interfaces, 2013, 5, 2745-2751.	8.0	66
262	CO Oxidation on Colloidal Au _{0.80} Pd _{0.20} –Fe _{<i>x</i>} O _{<i>y</i>} Dumbbell Nanocrystals. Nano Letters, 2013, 13, 752-757.	9.1	57
263	Highly luminescent, flexible and biocompatible cadmium-based nanocomposites. Microelectronic Engineering, 2013, 111, 299-303.	2.4	2
264	Colloidal Ordered Assemblies in a Polymer Shell—A Novel Type of Magnetic Nanobeads for Theranostic Applications. Chemistry of Materials, 2013, 25, 1055-1062.	6.7	56
265	Plasmon Dynamics in Colloidal Au ₂ Cd Alloy–CdSe Core/Shell Nanocrystals. ACS Nano, 2013, 7, 1045-1053.	14.6	33
266	Compression stiffness of porous nanostructures from self-assembly of branched nanocrystals. Nanoscale, 2013, 5, 681-686.	5.6	8
267	Atomic Ligand Passivation of Colloidal Nanocrystal Films via their Reaction with Propyltrichlorosilane. Chemistry of Materials, 2013, 25, 1423-1429.	6.7	30
268	Two-Photon-Induced Blue Shift of Core and Shell Optical Transitions in Colloidal CdSe/CdS Quasi-Type II Quantum Rods. ACS Nano, 2013, 7, 2443-2452.	14.6	46
269	Subnanometer Local Temperature Probing and Remotely Controlled Drug Release Based on Azo-Functionalized Iron Oxide Nanoparticles. Nano Letters, 2013, 13, 2399-2406.	9.1	351
270	Colloidal Branched Semiconductor Nanocrystals: State of the Art and Perspectives. Accounts of Chemical Research, 2013, 46, 1387-1396.	15.6	94

#	Article	IF	CITATIONS
271	Colloidal CdSe/Cu ₃ P/CdSe Nanocrystal Heterostructures and Their Evolution upon Thermal Annealing. ACS Nano, 2013, 7, 3997-4005.	14.6	36
272	Phase diagram of octapod-shaped nanocrystals in a quasi-two-dimensional planar geometry. Journal of Chemical Physics, 2013, 138, 154504.	3.0	16
273	Optical Properties of Semiconductor Nanorods. Nanoscience and Technology, 2013, , 7-55.	1.5	3
274	Hybrid Lasers Based on CdSe/CdS Core/Shell Colloidal Quantum Rods on Silica Microspheres. , 2012, , .		0
275	Influence of Chloride Ions on the Synthesis of Colloidal Branched CdSe/CdS Nanocrystals by Seeded Growth. ACS Nano, 2012, 6, 11088-11096.	14.6	64
276	Effect of Morphology on Ultrafast Carrier Dynamics in Asymmetric Gold–Iron Oxide Plasmonic Heterodimers. Journal of Physical Chemistry C, 2012, 116, 26924-26928.	3.1	11
277	Spatial analysis of the photocurrent generation and transport in semiconductor nanocrystal films. Physical Review B, 2012, 86, .	3.2	7
278	Light-Induced Inhibition of Photoluminescence Emission of Core/Shell Semiconductor Nanorods and Its Application for Optical Data Storage. Journal of Physical Chemistry C, 2012, 116, 25576-25580.	3.1	6
279	Ordered Two-Dimensional Superstructures of Colloidal Octapod-Shaped Nanocrystals on Flat Substrates. Nano Letters, 2012, 12, 5299-5303.	9.1	55
280	A Roadmap for the Assembly of Polyhedral Particles. Science, 2012, 337, 417-418.	12.6	16
281	Spinning nanorods – active optical manipulation of semiconductor nanorods using polarised light. Nanoscale, 2012, 4, 3693.	5.6	20
282	Colloidal Cu2â^'x(SySe1â^'y) alloy nanocrystals with controllable crystal phase: synthesis, plasmonic properties, cation exchange and electrochemical lithiation. Journal of Materials Chemistry, 2012, 22, 13023.	6.7	70
283	A superbright X-ray laboratory microsource empowered by a novel restoration algorithm. Journal of Applied Crystallography, 2012, 45, 1228-1235.	4.5	23
284	Editorial: Plasmonic sensors. Annalen Der Physik, 2012, 524, A155-A155.	2.4	0
285	Strongly Fluorescent Quaternary Cu–In–Zn–S Nanocrystals Prepared from Cu _{1-<i>x</i>} InS ₂ Nanocrystals by Partial Cation Exchange. Chemistry of Materials, 2012, 24, 2400-2406.	6.7	291
286	Novel hybrid organic/inorganic 2D photonic quasicrystals with 8-fold and 12-fold diffraction symmetries. , 2012, , .		1
287	Thermally Induced Structural and Morphological Changes of CdSe/CdS Octapods. Small, 2012, 8, 937-942.	10.0	21
288	Water-Soluble Iron Oxide Nanocubes with High Values of Specific Absorption Rate for Cancer Cell Hyperthermia Treatment. ACS Nano, 2012, 6, 3080-3091.	14.6	638

#	Article	IF	CITATIONS
289	Charge Transport in Nanoscale "All-Inorganic―Networks of Semiconductor Nanorods Linked by Metal Domains. ACS Nano, 2012, 6, 2940-2947.	14.6	46
290	Plasmon Bleaching Dynamics in Colloidal Gold–Iron Oxide Nanocrystal Heterodimers. Nano Letters, 2012, 12, 921-926.	9.1	32
291	Size-Tunable, Hexagonal Plate-like Cu ₃ P and Janus-like Cu–Cu ₃ P Nanocrystals. ACS Nano, 2012, 6, 32-41.	14.6	94
292	Selfâ€assembled CdSe/CdS nanorod microâ€lasers fabricated from solution by capillary jet deposition. Laser and Photonics Reviews, 2012, 6, 678-683.	8.7	47
293	Understanding the Plasmon Resonance in Ensembles of Degenerately Doped Semiconductor Nanocrystals. Journal of Physical Chemistry C, 2012, 116, 12226-12231.	3.1	109
294	Blue-UV-Emitting ZnSe(Dot)/ZnS(Rod) Core/Shell Nanocrystals Prepared from CdSe/CdS Nanocrystals by Sequential Cation Exchange. ACS Nano, 2012, 6, 1637-1647.	14.6	138
295	Band-edge ultrafast pump–probe spectroscopy of core/shell CdSe/CdS rods: assessing electron delocalization by effective mass calculations. Physical Chemistry Chemical Physics, 2012, 14, 7420.	2.8	12
296	Direct Determination of Polarity, Faceting, and Core Location in Colloidal Core/Shell Wurtzite Semiconductor Nanocrystals. ACS Nano, 2012, 6, 6453-6461.	14.6	61
297	Colloidal Inorganic Nanocrystals. , 2012, , 251-281.		Ο
298	Spatially resolved photoconductivity of thin films formed by colloidal octapod-shaped CdSe/CdS nanocrystals. Nanoscale, 2011, 3, 2964.	5.6	10
299	Assembly of shape-controlled nanocrystals by depletion attraction. Chemical Communications, 2011, 47, 203-205.	4.1	64
300	Steady-state photoinduced absorption of CdSe/CdS octapod shaped nanocrystals. Physical Chemistry Chemical Physics, 2011, 13, 15326.	2.8	9
301	Chemically induced self-assembly of spherical and anisotropic inorganic nanocrystals. Journal of Materials Chemistry, 2011, 21, 16694.	6.7	45
302	Luminescent Solar Concentrators utilising aligned CdSe/CdS nanorods. , 2011, , .		3
303	Ultrafast carrier dynamics in gold/iron-oxide nanocrystal heterodimers. Applied Physics Letters, 2011, 99, 011907.	3.3	18
304	Birth and Growth of Octapod-Shaped Colloidal Nanocrystals Studied by Electron Tomography. Journal of Physical Chemistry C, 2011, 115, 20128-20133.	3.1	18
305	Ultrafast Exciton Dynamics in Colloidal CdSe/CdS Octapod Shaped Nanocrystals. Journal of Physical Chemistry C, 2011, 115, 9005-9011.	3.1	19
306	A Cast-Mold Approach to Iron Oxide and Pt/Iron Oxide Nanocontainers and Nanoparticles with a Reactive Concave Surface. Journal of the American Chemical Society, 2011, 133, 2205-2217.	13.7	71

#	Article	IF	CITATIONS
307	Temperature and Size Dependence of the Optical Properties of Tetrapod-Shaped Colloidal Nanocrystals Exhibiting Type-II Transitions. Journal of Physical Chemistry C, 2011, 115, 18094-18104.	3.1	17
308	Cation Exchange Reactions in Colloidal Branched Nanocrystals. ACS Nano, 2011, 5, 7176-7183.	14.6	110
309	Chemical Transformation of Au-Tipped CdS Nanorods into AuS/Cd Core/Shell Particles by Electron Beam Irradiation. Nano Letters, 2011, 11, 4555-4561.	9.1	33
310	Amplified spontaneous emission from core and shell transitions in CdSe/CdS nanorods fabricated by seeded growth. Applied Physics Letters, 2011, 98, .	3.3	35
311	Charge Transport and Electrochemical Properties of Colloidal Greigite (Fe ₃ S ₄) Nanoplatelets. Chemistry of Materials, 2011, 23, 3762-3768.	6.7	60
312	Multifunctional Nanobeads Based on Quantum Dots and Magnetic Nanoparticles: Synthesis and Cancer Cell Targeting and Sorting. ACS Nano, 2011, 5, 1109-1121.	14.6	166
313	Sequential Cation Exchange in Nanocrystals: Preservation of Crystal Phase and Formation of Metastable Phases. Nano Letters, 2011, 11, 4964-4970.	9.1	300
314	Reversible Tunability of the Near-Infrared Valence Band Plasmon Resonance in Cu _{2–<i>x</i>} Se Nanocrystals. Journal of the American Chemical Society, 2011, 133, 11175-11180.	13.7	421
315	Optical and electrical properties of colloidal (spherical Au)-(spinel ferrite nanorod) heterostructures. Nanoscale, 2011, 3, 4647.	5.6	21
316	Plasmon Dynamics in Colloidal Cu _{2–<i>x</i>} Se Nanocrystals. Nano Letters, 2011, 11, 4711-4717.	9.1	158
317	Novel hybrid organic/inorganic 2D quasiperiodic PC: from diffraction pattern to vertical light extraction. Nanoscale Research Letters, 2011, 6, 371.	5.7	16
318	Hierarchical self-assembly of suspended branched colloidal nanocrystals into superlattice structures. Nature Materials, 2011, 10, 872-876.	27.5	415
319	Physical properties of elongated inorganic nanoparticles. Physics Reports, 2011, 501, 75-221.	25.6	138
320	Selfâ€Assembled Multilayers of Vertically Aligned Semiconductor Nanorods on Deviceâ€6cale Areas. Advanced Materials, 2011, 23, 2205-2209.	21.0	83
321	A novel hybrid organic/inorganic photonic crystal slab showing a resonance action at the band edge. Nanotechnology, 2011, 22, 285307.	2.6	11
322	Fabrication and spectroscopic studies on highly luminescent CdSe/CdS nanorod polymer composites. Beilstein Journal of Nanotechnology, 2010, 1, 94-100.	2.8	61
323	Photoconduction Properties in Aligned Assemblies of Colloidal CdSe/CdS Nanorods. ACS Nano, 2010, 4, 1646-1652.	14.6	73
324	Electron microscopy studies of electronâ€beam sensitive PbTeâ€based nanostructures. Microscopy Research and Technique, 2010, 73, 944-951.	2.2	2

2

#	Article	IF	CITATIONS
325	Optically induced light modulation in an hybrid nanocomposite system of inorganic CdSe/CdS nanorods and nematic liquid crystals. Optical Materials, 2010, 32, 1011-1016.	3.6	31
326	Dynamic orientational photorefractive gratings observed in CdSe/CdS nanorods imbedded in liquid crystal cells. Optical Materials, 2010, 32, 1060-1065.	3.6	4
327	Dots in rods as polarized single photon sources. Superlattices and Microstructures, 2010, 47, 165-169.	3.1	37
328	Evidence for an internal field in CdSe/CdS nanorods by time resolved and single rod experiments. Superlattices and Microstructures, 2010, 47, 174-177.	3.1	5
329	Evidence of electron wave function delocalization in CdSe/CdS asymmetric nanocrystals. Superlattices and Microstructures, 2010, 47, 170-173.	3.1	10
330	DYNAMIC ORIENTATIONAL PHOTO-REFRACTIVE GRATINGS OBSERVED IN CdSe/CdS NANORODS DOPED NEMATIC LIQUID CRYSTAL CELLS. Journal of Nonlinear Optical Physics and Materials, 2010, 19, 111-121.	1.8	3
331	Assembly of Colloidal Semiconductor Nanorods in Solution by Depletion Attraction. Nano Letters, 2010, 10, 743-749.	9.1	250
332	Room temperature-dipolelike single photon source with a colloidal dot-in-rod. Applied Physics Letters, 2010, 96, 033101.	3.3	75
333	From iron oxide nanoparticles towards advanced iron-based inorganic materials designed for biomedical applications. Pharmacological Research, 2010, 62, 126-143.	7.1	417
334	Suppression of Biexciton Auger Recombination in CdSe/CdS Dot/Rods: Role of the Electronic Structure in the Carrier Dynamics. Nano Letters, 2010, 10, 3142-3150.	9.1	97
335	Epitaxial CdSe-Au Nanocrystal Heterostructures by Thermal Annealing. Nano Letters, 2010, 10, 3028-3036.	9.1	152
336	Octapod-Shaped Colloidal Nanocrystals of Cadmium Chalcogenides via "One-Pot―Cation Exchange and Seeded Growth. Nano Letters, 2010, 10, 3770-3776.	9.1	171
337	Acidic pH-Responsive Nanogels as Smart Cargo Systems for the Simultaneous Loading and Release of Short Oligonucleotides and Magnetic Nanoparticles. Langmuir, 2010, 26, 10315-10324.	3.5	54
338	Phosphine-Free Synthesis of p-Type Copper(I) Selenide Nanocrystals in Hot Coordinating Solvents. Journal of the American Chemical Society, 2010, 132, 8912-8914.	13.7	232
339	Lasing in self-assembled microcavities of CdSe/CdS core/shell colloidal quantum rods. Nanoscale, 2010, 2, 931.	5.6	120
340	Colloidal PbTe–Aunanocrystal heterostructures. Journal of Materials Chemistry, 2010, 20, 1357-1366.	6.7	46
341	Phototransport in networks of tetrapod-shaped colloidal semiconductor nanocrystals. Nanoscale, 2010, 2, 2171.	5.6	28

Luminescent Solar Concentrators. , 2010, , 323-349.

#	Article	IF	CITATIONS
343	Improved photovoltaic performance of bilayer heterojunction photovoltaic cells by triplet materials and tetrapod-shaped colloidal nanocrystals doping. Applied Physics Letters, 2009, 95, 043101.	3.3	20
344	An <i>ab initio</i> study of the magnetic–metallic CoPt ₃ –Au interfaces. Journal of Physics Condensed Matter, 2009, 21, 015001.	1.8	1
345	Endâ€ŧoâ€End Assembly of Shapeâ€Controlled Nanocrystals via a Nanowelding Approach Mediated by Gold Domains. Advanced Materials, 2009, 21, 550-554.	21.0	114
346	Improved Photovoltaic Performance of Heterostructured Tetrapodâ€ S haped CdSe/CdTe Nanocrystals Using C60 Interlayer. Advanced Materials, 2009, 21, 4461-4466.	21.0	58
347	Magnetic–Fluorescent Colloidal Nanobeads: Preparation and Exploitation in Cell Separation Experiments. Macromolecular Bioscience, 2009, 9, 952-958.	4.1	66
348	Selfâ€Assembly of Amphiphilic Nanocrystals. Angewandte Chemie - International Edition, 2009, 48, 4282-4283.	13.8	18
349	Polarized single photon emission for quantum cryptography based on colloidal nanocrystals. , 2009, ,		3
350	Self-assembly of highly fluorescent semiconductor nanorods into large scale smectic liquid crystal structures by coffee stain evaporation dynamics. Journal of Physics Condensed Matter, 2009, 21, 264013.	1.8	42
351	Polarized Light Emitting Diode by Long-Range Nanorod Self-Assembling on a Water Surface. ACS Nano, 2009, 3, 1506-1512.	14.6	127
352	Fluorescent Asymmetrically Cobalt-Tipped CdSe@CdS Core@Shell Nanorod Heterostructures Exhibiting Room-Temperature Ferromagnetic Behavior. Journal of the American Chemical Society, 2009, 131, 12817-12828.	13.7	119
353	CdSe/CdS/ZnS Double Shell Nanorods with High Photoluminescence Efficiency and Their Exploitation As Biolabeling Probes. Journal of the American Chemical Society, 2009, 131, 2948-2958.	13.7	247
354	Tetrapod-Shaped Colloidal Nanocrystals of Ilâ^'VI Semiconductors Prepared by Seeded Growth. Journal of the American Chemical Society, 2009, 131, 2274-2282.	13.7	211
355	Ultrafast carrier dynamics in spherical CdSe core/elongated CdS shell nanocrystals. Springer Series in Chemical Physics, 2009, , 289-291.	0.2	1
356	Fluorescent Nanocrystals and Proteins. Nanostructure Science and Technology, 2009, , 225-254.	0.1	0
357	Determination of surface properties of various substrates using TiO2 nanorod coatings with tunable characteristics. Journal of Materials Science, 2008, 43, 3474-3480.	3.7	14
358	Rodâ€Shaped Nanocrystals Elicit Neuronal Activity In Vivo. Small, 2008, 4, 1747-1755.	10.0	38
359	Probe Tips Functionalized with Colloidal Nanocrystal Tetrapods for Highâ€Resolution Atomic Force Microscopy Imaging. Small, 2008, 4, 2123-2126.	10.0	19
360	Role of defect states on electrical and optical properties in CdSe nanorod thin films. Physica E: Low-Dimensional Systems and Nanostructures, 2008, 40, 2063-2065.	2.7	2

#	Article	IF	CITATIONS
361	Magnetic properties of novel superparamagnetic MRI contrast agents based on colloidal nanocrystals. Journal of Magnetism and Magnetic Materials, 2008, 320, e320-e323.	2.3	45
362	Shell thickness dependence of exciton trapping in colloidal core/shell nanorods. Journal of Luminescence, 2008, 128, 361-365.	3.1	5
363	The influence of intrinsic and surface states on the emission properties of colloidal nanocrystals. Superlattices and Microstructures, 2008, 43, 528-531.	3.1	2
364	Interconnection of specific nano-objects by electron beam lithography — A controllable method. Materials Science and Engineering C, 2008, 28, 299-302.	7.3	2
365	Ultrafast Electronâ~'Hole Dynamics in Core/Shell CdSe/CdS Dot/Rod Nanocrystals. Nano Letters, 2008, 8, 4582-4587.	9.1	146
366	Growth mechanism, shape and composition control of semiconductor nanocrystals. , 2008, , 1-34.		7
367	One-Pot Synthesis and Characterization of Size-Controlled Bimagnetic FePtâ^'Iron Oxide Heterodimer Nanocrystals. Journal of the American Chemical Society, 2008, 130, 1477-1487.	13.7	179
368	Reversible Wettability Changes in Colloidal TiO ₂ Nanorod Thin-Film Coatings under Selective UV Laser Irradiation. Journal of Physical Chemistry C, 2008, 112, 701-714.	3.1	96
369	Ligand exchange of CdSe nanocrystals probed by optical spectroscopy in the visible and mid-IR. Journal of Materials Chemistry, 2008, 18, 2728.	6.7	71
370	Water solubilization of hydrophobic nanocrystals by means of poly(maleic) Tj ETQq0 0 0 rgBT /Overlock 10 Tf 50	382 Td (a 6.7	nhydride-alt- 133
371	Determination of Band Offsets in Heterostructured Colloidal Nanorods Using Scanning Tunneling Spectroscopy. Nano Letters, 2008, 8, 2954-2958.	9.1	179
372	Growth of colloidal nanoparticles of group Il–VI and IV–VI semiconductors on top of magnetic iron–platinum nanocrystals. Journal of Materials Chemistry, 2008, 18, 4311.	6.7	49
373	Two-Dimensional Photonic Crystal Resist Membrane Nanocavity Embedding Colloidal Dot-in-a-Rod Nanocrystals. Nano Letters, 2008, 8, 260-264.	9.1	38
374	Multifunctional Nanostructures Based on Inorganic Nanoparticles and Oligothiophenes and Their Exploitation for Cellular Studies. Journal of the American Chemical Society, 2008, 130, 10545-10555.	13.7	98
375	Radiative recombination dynamics in tetrapod-shaped CdTe nanocrystals: Evidence for a photoinduced screening of the internal electric field. Applied Physics Letters, 2008, 92, .	3.3	7
376	Intrinsic optical nonlinearity in colloidal seeded grown CdSe/CdS nanostructures: Photoinduced screening of the internal electric field. Physical Review B, 2008, 78, .	3.2	91
377	Role of defect states on Auger processes in resonantly pumped CdSe nanorods. Applied Physics Letters, 2007, 91, 093106.	3.3	9
378	Synthetic Strategies to Size and Shape Controlled Nanocrystals and Nanocrystal Heterostructures. Advances in Experimental Medicine and Biology, 2007, 620, 1-17.	1.6	7

#	Article	IF	CITATIONS
379	Synthesis and Micrometer-Scale Assembly of Colloidal CdSe/CdS Nanorods Prepared by a Seeded Growth Approach. Nano Letters, 2007, 7, 2942-2950.	9.1	1,098
380	Temperature and Size Dependence of Nonradiative Relaxation and Excitonâ´'Phonon Coupling in Colloidal CdTe Quantum Dots. Journal of Physical Chemistry C, 2007, 111, 5846-5849.	3.1	144
381	Confined Optical Phonon Modes in Aligned Nanorod Arrays Detected by Resonant Inelastic Light Scattering. Nano Letters, 2007, 7, 476-479.	9.1	46
382	Picosecond Photoluminescence Decay Time in Colloidal Nanocrystals:  The Role of Intrinsic and Surface States. Journal of Physical Chemistry C, 2007, 111, 10541-10545.	3.1	46
383	Topologically Controlled Growth of Magnetic-Metal-Functionalized Semiconductor Oxide Nanorods. Nano Letters, 2007, 7, 1386-1395.	9.1	155
384	Synthesis and Biological Assay of GSH Functionalized Fluorescent Quantum Dots for StainingHydra vulgaris. Bioconjugate Chemistry, 2007, 18, 829-835.	3.6	52
385	Semiconductor Quantum Rods as Single Molecule Fluorescent Biological Labels. Nano Letters, 2007, 7, 179-182.	9.1	180
386	Blue light emitting diodes based on fluorescent CdSeâ^•ZnS nanocrystals. Applied Physics Letters, 2007, 90, 051106.	3.3	82
387	Fluorescent-Magnetic Hybrid Nanostructures: Preparation, Properties, and Applications in Biology. IEEE Transactions on Nanobioscience, 2007, 6, 298-308.	3.3	96
388	Sequential Growth of Magic-Size CdSe Nanocrystals. Advanced Materials, 2007, 19, 548-552.	21.0	289
389	Catalytic and seeded shape-selective synthesis of II–VI semiconductor nanowires. Physica E: Low-Dimensional Systems and Nanostructures, 2007, 37, 138-141.	2.7	7
390	Synthesis routes for the growth of complex nanostructures. Physica E: Low-Dimensional Systems and Nanostructures, 2007, 37, 128-133.	2.7	14
391	Fluorescence enhancement in colloidal semiconductor nanocrystals by metallic nanopatterns. Sensors and Actuators B: Chemical, 2007, 126, 187-192.	7.8	34
392	Confinement effects on optical phonons in spherical, rod-, and tetrapod-shaped nanocrystals detected by Raman spectroscopy. Physica Status Solidi (A) Applications and Materials Science, 2007, 204, 483-486.	1.8	16
393	The Role of Intrinsic and Surface States on the Emission Properties of Colloidal CdSe and CdSe/ZnS Quantum Dots. Nanoscale Research Letters, 2007, 2, 512-514.	5.7	20
394	Exciton transitions in tetrapod-shaped CdTe nanocrystals investigated by photomodulated transmittance spectroscopy. Applied Physics Letters, 2006, 89, 094104.	3.3	10
395	Selective reactions on the tips of colloidal semiconductor nanorods. Journal of Materials Chemistry, 2006, 16, 3952.	6.7	108
396	Confinement Effects on Optical Phonons in Polar Tetrapod Nanocrystals Detected by Resonant Inelastic Light Scattering. Nano Letters, 2006, 6, 478-482.	9.1	35

#	Article	IF	CITATIONS
397	Multiple Wurtzite Twinning in CdTe Nanocrystals Induced by Methylphosphonic Acid. Journal of the American Chemical Society, 2006, 128, 748-755.	13.7	165
398	Synthesis, properties and perspectives of hybrid nanocrystal structures. Chemical Society Reviews, 2006, 35, 1195.	38.1	855
399	Electronâ^'Hole Dynamics in CdTe Tetrapods. Journal of Physical Chemistry B, 2006, 110, 17334-17338.	2.6	37
400	Heterodimers Based on CoPt3â^'Au Nanocrystals with Tunable Domain Size. Journal of the American Chemical Society, 2006, 128, 6690-6698.	13.7	202
401	Synthesis and perspectives of complex crystalline nano-structures. Physica Status Solidi (A) Applications and Materials Science, 2006, 203, 1329-1336.	1.8	10
402	Metal-enhanced fluorescence of colloidal nanocrystals with nanoscale control. Nature Nanotechnology, 2006, 1, 126-130.	31.5	573
403	Fluorescence resonance energy transfer induced by conjugation of metalloproteins to nanoparticles. Chemical Physics Letters, 2006, 417, 351-357.	2.6	22
404	Colloidal Synthesis and Characterization of Tetrapod-Shaped Magnetic Nanocrystals. Nano Letters, 2006, 6, 1966-1972.	9.1	140
405	High Q-factor colloidal nanocrystal-based vertical microcavity by hot embossing technology. Applied Physics Letters, 2006, 88, 181108.	3.3	19
406	Role of the shell thickness in stimulated emission and photoinduced absorption inCdSecore/shell nanorods. Physical Review B, 2006, 73, .	3.2	39
407	Shape Dependence of the Scattering Processes of Optical Phonons in Colloidal Nanocrystals Detected by Raman Spectroscopy. Journal of Nanoelectronics and Optoelectronics, 2006, 1, 104-107.	0.5	6
408	Tailoring the emission spectrum of colloidal nanocrystals by means of lithographically-imprinted hybrid vertical microcavities. , 2005, 5840, 168.		2
409	Optical properties of colloidal nanocrystal spheres and tetrapods. Microelectronics Journal, 2005, 36, 552-554.	2.0	11
410	Formation and characterization of glutamate dehydrogenase monolayers on silicon supports. Biosensors and Bioelectronics, 2005, 21, 30-40.	10.1	12
411	Tips on growing nanocrystals. Nature Materials, 2005, 4, 801-802.	27.5	55
412	Precipitation of Selenium from CdSe Nanocrystal Solutions. Advanced Materials, 2005, 17, 1321-1324.	21.0	7
413	Ultrafast carrier dynamics in core and core/shell CdSe quantum rods: Role of the surface and interface defects. Physical Review B, 2005, 72, .	3.2	72
414	Optical properties of tetrapod-shaped CdTe nanocrystals. Applied Physics Letters, 2005, 87, 224101.	3.3	44

#	Article	IF	CITATIONS
415	Shape and Phase Control of Colloidal ZnSe Nanocrystals. Chemistry of Materials, 2005, 17, 1296-1306.	6.7	220
416	First-Principles Modeling of Unpassivated and Surfactant-Passivated Bulk Facets of Wurtzite CdSe:  A Model System for Studying the Anisotropic Growth of CdSe Nanocrystals. Journal of Physical Chemistry B, 2005, 109, 6183-6192.	2.6	280
417	Selective Growth of PbSe on One or Both Tips of Colloidal Semiconductor Nanorods. Nano Letters, 2005, 5, 445-449.	9.1	228
418	White organic light-emitting devices with CdSe/ZnS quantum dots as a red emitter. Journal of Applied Physics, 2005, 97, 113501.	2.5	115
419	Colloidal nanocrystal heterostructures with linear and branched topology. Nature, 2004, 430, 190-195.	27.8	1,127
420	The Effect of Organic Ligand Binding on the Growth of CdSe Nanoparticles Probed by Ab Initio Calculations. Nano Letters, 2004, 4, 2361-2365.	9.1	301
421	On the Development of Colloidal Nanoparticles towards Multifunctional Structures and their Possible Use for Biological Applications. Small, 2004, 1, 48-63.	10.0	353
422	A novel synthesis of CdSe nanocrystals. Materials Letters, 2004, 58, 2429-2432.	2.6	8
423	Förster energy transfer from blue-emitting polymers to colloidal CdSeâ^•ZnS core shell quantum dots. Applied Physics Letters, 2004, 85, 4169-4171.	3.3	142
424	Hydrophobic Nanocrystals Coated with an Amphiphilic Polymer Shell:Â A General Route to Water Soluble Nanocrystals. Nano Letters, 2004, 4, 703-707.	9.1	1,003
425	Title is missing!. Journal of Sol-Gel Science and Technology, 2003, 26, 441-446.	2.4	9
426	Controlled growth of tetrapod-branched inorganic nanocrystals. Nature Materials, 2003, 2, 382-385.	27.5	1,373
427	Exciton relaxation processes in colloidal core/shell ZnSe/ZnS nanocrystals. Applied Physics Letters, 2003, 82, 418-420.	3.3	48
428	Shape control and applications of nanocrystals. Philosophical Transactions Series A, Mathematical, Physical, and Engineering Sciences, 2003, 361, 241-257.	3.4	184
429	Epitaxial Growth and Photochemical Annealing of Graded CdS/ZnS Shells on Colloidal CdSe Nanorods. Journal of the American Chemical Society, 2002, 124, 7136-7145.	13.7	539
430	Semiconductor Nanorod Liquid Crystals. Nano Letters, 2002, 2, 557-560.	9.1	297
431	Shape Control of Colloidal Semiconductor Nanocrystals. Journal of Cluster Science, 2002, 13, 521-532.	3.3	142
432	Linearly Polarized Emission from Colloidal Semiconductor Quantum Rods. Science, 2001, 292, 2060-2063.	12.6	1,136

#	Article	IF	CITATIONS
433	Preparation and characterisation of organic–inorganic heterojunction based on BDA-PPV/CdS nanocrystals. Materials Science and Engineering B: Solid-State Materials for Advanced Technology, 2000, 74, 175-179.	3.5	12
434	Shape control of CdSe nanocrystals. Nature, 2000, 404, 59-61.	27.8	4,216
435	Synthesis and Characterization of CdS Nanoclusters in a Quaternary Microemulsion:  the Role of the Cosurfactant. Journal of Physical Chemistry B, 2000, 104, 8391-8397.	2.6	173
436	Synthesis of Soluble and Processable Rod-, Arrow-, Teardrop-, and Tetrapod-Shaped CdSe Nanocrystals. Journal of the American Chemical Society, 2000, 122, 12700-12706.	13.7	1,719
437	Quantum Dots. , 0, , 4-49.		2
438	A lithium ion battery exploiting a composite Fe2O3 anode and a high voltage Li1.35Ni0.48Fe0.1Mn1.72O4 cathode. RSC Advances, 0, , .	3.6	6
439	Nanoparticles and Nanostructures for Biophotonic Applications. , 0, , .		1